

# Estimating localization network node positions with a multi-robot system

Mikko Elomaa and Aarne Halme, *Member, IEEE*

**Abstract**—A novel method using bearing-only SLAM to estimate node positions of a localization network is proposed. A group of simple robots are used to estimate the position of each node. Each node has a unique ID, which it can communicate to a robot close by. Initially the node IDs and positions are unknown. A case example using RFID technology in the localization network is introduced.

**Index Terms**—Localization network, Multi-robot, RFID, SLAM

## I. INTRODUCTION

THE localization of a mobile robot is of paramount importance for efficient task execution. The field has been well studied and many different methods have been proposed. These methods can be roughly divided into two categories: methods relying only on robot's own sensors and methods using external infrastructure such as beacons, landmarks, etc. Each method has its benefits and short-comings. The choice depends on the application and environment, but some methods have proven to be more generally applicable. A common approach for robot localization is the method called Simultaneous Localization and Mapping (SLAM). It combines the measurements of the robots internal sensors with the observations of the environment. The detected features of the environment may be natural or artificial. No a priori information on the features is required. Several studies have addressed this method [1], [2], [3], [4], [5].

In multi-robot scenarios the robots can improve their position estimates by observing other robots. The localization can be based on other robots serving as static landmarks, while other robots move [6]. A simplified approach is to have two robots moving in turns. Only one robot needs to have necessary sensors for detecting the target mounted on the other robot [7]. A robot group can also move in a formation, while the robots observe each other continuously [8], [9]. Both approaches have the restriction, that the robots have to stay together in order to observe each other. This can be inconvenient in many scenarios. Cooperation between robots navigating independently has also been studied. For example, the SLAM method can be extended to handle multi-robot cooperation [10], [11], [12], [13], [14].

If the pose estimate of a robot is based only on the measurements of relative change in the pose, the uncertainty of the estimate increases over time. In SLAM the robot also observes its environment in order to have measurements from external objects. This is often done with a laser scanner and has been

shown to work well in some environments. However, problems arise, when the environment does not provide features, that can be identified or if a large error is introduced into the pose estimate of the robot. With an external localization network, a robot can always localize itself within a bounded error. If landmarks with unique identification codes are used, the robot detecting a landmark has no correspondence problem. The measurements to landmarks together with the position estimates of the landmarks can be used to compute a position estimate for the robot. The accuracy of the position estimate is independent of time. The problem is that the deployment and maintenance of the localization network is often costly.

The approach introduced in this paper uses a group of simple robots with basic sensors for estimation of landmark positions. Hence, no costly deployment with accurate initial localization of landmarks is needed. Each robot only needs wheel encoders and one sensor, that can identify a landmark and measure a bearing angle to the landmark. With these sensors, the robots are able to estimate simultaneously their own pose and the locations of the landmarks in the localization network. The landmarks can be deployed sparsely because only one landmark needs to be visible for the localization algorithm to work. If no landmark is visible, the robot relies entirely on the odometry.

Human operated platforms with odometry sensors could also be used for the localization of the landmarks instead of the robots. The platforms could be pushed or teleoperated according to the operating environment. The human participation may be feasible in an environment, where the autonomous navigation of a robot without complex sensor system is difficult or where human entities are needed for specific tasks.

A case example introduced in this paper shows, that maintenance free, passive RFID tags can be used as landmarks for a SLAM application. The use of passive RFID technology for localization has been studied earlier in several separate research projects. In [15], [16] the RFID tags are used to identify sub maps, but the actual localization is done with other sensors. In [17], [18] an excessive amount of tags is used to cover the floor and the localization is based on detection of a tag directly below the robot. In [19] passive RFID tags are used as landmarks. A robot with two static antennas detect the tags on the walls of an office space and create a map of them using a probabilistic algorithm. The pose estimate of the robot localizing the landmarks is based on separate system. Thus, the method presented is not an application of SLAM.

M. Elomaa and A. Halme are with the Department of Automation and Systems Technology, Aalto University, Helsinki, Finland e-mail: (see <http://autsys.tkk.fi/en/Staff/Automation>).

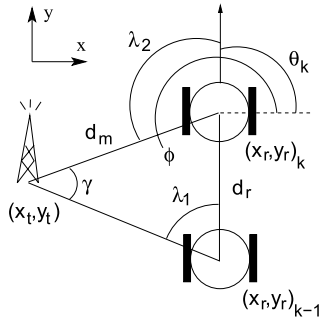


Fig. 1. Landmark localization with two bearing angle measurements.

## II. BEARING-ONLY SLAM

If the robot can measure at least two bearing angles to a landmark, an estimate can be calculated for the relative displacement between the landmark and the robot, provided that the robot has basic odometry sensors. An estimate for the relative position of the landmark can be found at the intersection of the two bearing angle measurements.

Figure 1 shows a robot making two bearing angle measurements at locations  $R_k$  and  $R_{k+1}$ . The distance  $d_r$  between the two locations is measured with wheel encoders. The two bearing angle measurements  $\lambda_1$  and  $\lambda_2$  are measured with a suitable sensor. The displacement relative to the position of the robot can be calculated in polar coordinates as follows:

$$\phi = \theta + \lambda_2 \quad (1)$$

$$d_m = \frac{d_r \cdot \sin(\lambda_1)}{\sin(\lambda_2 - \lambda_1)} \quad (2)$$

Extended Kalman Filter (EKF) can be used to estimate the pose of the robot and the position of a landmark based on a measured bearing angle and existing estimates of the robot pose and landmark position. An example state vector with a robot pose and a landmark position estimates and a control vector defining the robot movement are as follows:

$$\hat{x} = \begin{bmatrix} \hat{x}_r \\ \hat{y}_r \\ \hat{\theta} \\ \hat{x}_t \\ \hat{y}_t \end{bmatrix} \quad u = \begin{bmatrix} d \\ \psi \\ \Delta\theta \\ 0 \\ 0 \end{bmatrix}$$

At the prediction step the change in the pose of the robot is estimated according to the information received from the odometry system (Figure 2). The information related to the pose change is considered as external control  $u_k$ . The predicted pose of the robot is computed according to the function  $f(x_{k-1}, u_k, 0)$  containing the Equations 3-5. The position of a landmark is static and thus its estimate does not change during the prediction step.

$$\hat{x}_{r,k}^- = \hat{x}_{r,k-1} + d_k \cdot \cos(\hat{\theta}_{k-1} + \psi_k) \quad (3)$$

$$\hat{y}_{r,k}^- = \hat{y}_{r,k-1} + d_k \cdot \sin(\hat{\theta}_{k-1} + \psi_k) \quad (4)$$

$$\hat{\theta}_k^- = \hat{\theta}_{k-1} + \Delta\theta \quad (5)$$

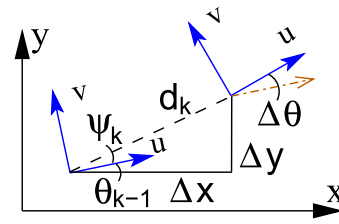


Fig. 2. Change in the robot pose as measured by the odometry system

The error covariance matrix  $P$  is updated at the prediction step according to the Equation 6, where  $A$  is a Jacobian matrix of partial derivatives  $\frac{\partial f}{\partial x}$  and  $B$  is a Jacobian matrix  $\frac{\partial f}{\partial u}$ .  $U_k$  is the noise covariance matrix for the external control and  $Q_k$  is a covariance matrix containing the process noise.

$$P_k^- = A_k P_{k-1} A_k^T + B_k U_k B_k^T + Q_k \quad (6)$$

The measured bearing angle is used to correct the predicted values of the state vector. The measurement equation  $h(\hat{x}_k^-, 0)$  is described in Equation 7. The correction for the state vector is calculated using the Kalman gain parameter, which for EKF has to be computed for each step as it depends on the linearization at the current state. The Kalman gain is computed according to the Equation 8, where  $H$  is a Jacobian matrix  $\frac{\partial h}{\partial x}$  and  $R_k$  is the measurement noise covariance matrix. A residual of the measured bearing angle  $z_k$  and the predicted bearing angle, computed with measurement equation  $h$ , is calculated. The Kalman gain is used to weight the residual to each variable in the state vector (Equation 9). The error covariance matrix is updated using the Kalman gain and the Jacobian matrix  $H_k$ .

$$h(\hat{x}_k^-, 0) = \text{atan2} \left( \frac{\hat{y}_{t,k}^- - \hat{y}_{r,k}^-}{\hat{x}_{t,k}^- - \hat{x}_{r,k}^-} \right) - \hat{\theta}_k \quad (7)$$

$$K_k = P_k^- H_k^T (H_k P_k^- H_k^T + R_k)^{-1} \quad (8)$$

$$\hat{x}_k = \hat{x}_k^- + K_k (z_k - h(\hat{x}_k^-, 0)) \quad (9)$$

$$P_k = (I - K_k H_k) P_k^- \quad (10)$$

## III. COOPERATION

When a single robot estimates the position of a landmark the estimate is biased by the errors in the robot's own position and heading angle estimate. Filtering the different measurements of a single robot helps to decrease the effect of measurement errors, but not the effect of the error in the robot's original pose estimate. However, if different robots are estimating the position of a landmark, the position estimate is based on several more or less independent groups of measurements. The poses of different robots get correlated, when they use same landmarks for localization. This helps to keep the pose error of a robot on lower level in the early stages of the network node localization, as the other robots can offer it more accurate position estimates of the landmarks the robot has already localized (Figure 3). On the other hand, as the variables of the state vector get strongly correlated over time less and less new information is available and the location estimates

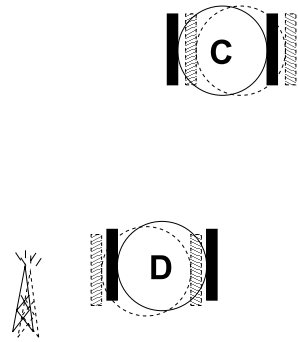


Fig. 3. Robot D passing the landmark and informing the robot C of the new position estimate of the landmark, that C has already passed. Both C and D correct their position.

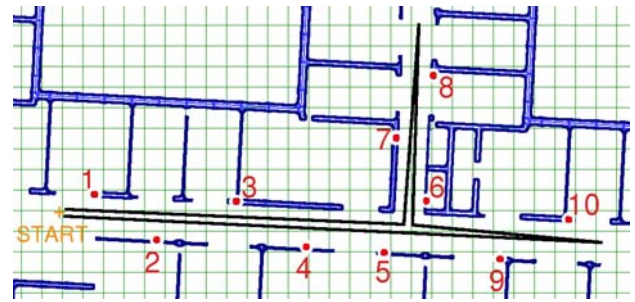


Fig. 4. The locations of the 10 landmarks and the approximate path followed by robots during the test runs

Open Science Index, Mechanical and Mechatronics Engineering Vol:4, No:8, 2010 publications.waset.org/7801/pdf

of the landmarks will become static. At the mature state of the localization network the cooperation between robots is no more needed for localization. The landmarks will provide a common frame of reference for all the robots operating on the area of the coverage.

A straightforward way of maintaining all the correlations is to use a centralized Kalman filter. Then the state vector will include pose estimates of all robots and position estimates of all landmarks. A system with  $M$  robots and  $N$  landmarks has  $3*M+2N$  elements in the state vector. In large scale systems the dimensions of the centralized Kalman filter may grow too big for efficient computation of the updates. Then a distributed or sparse filter structure may be used. In these experiments the dimensions stayed below a hundred and the computational burden was still manageable with a centralized filter. The use of centralized Kalman filter also requires, that each robot can communicate with the central computer running the filter. Depending on the environment this may be achieved with access points or with an ad-hoc network. If sufficient level of communication can not be obtained, a distributed filter structure has to be used. If the landmarks have accessible memory, they can be used for the information exchange between the robots. However, the cooperation between robots is less efficient, when all the information is not available to all robots.

#### IV. CASE EXAMPLE: PASSIVE RFID TAGS AS LANDMARKS

Simulations and laboratory experiments were used to test the feasibility of the introduced concept. The laboratory experiments were conducted in an office environment. The test environment consisted of a main corridor, side corridor and rooms (Figure 4). The dimensions of the used environment were approximately 30m x 15m. The floor material is smooth vinyl with good friction. Ten passive RFID (Radio Frequency Identification) tags were placed on the walls of the two corridors to act as landmarks with unique IDs.

Four small differential drive robots were used to gather measurement data. The robots were equipped with wheel encoders. A motor controller estimated the pose of a robot based on the encoder pulses. The odometry was found relatively accurate in the office environment. However, the wheelbase of the robots



Fig. 5. Four MarsuBot robots used in the laboratory experiments. Directional RFID antenna on top of each robot. An RFID tag serving as a landmark can be seen on the background.

was only 17cm, which makes the heading angle estimate of the robot prone to error.

Each robot was also equipped with an RFID reader and a directional antenna mounted on a hobby servo (Figure 5). The RFID reader operates on the UHF frequency range (approximately 867MHz in Europe). The bearing angle measurement to a passive RFID tag serving as a landmark was done by turning the reader antenna on small steps. The electric field of the directional antenna swept over the surroundings of the robot and powered the tag only, when it was pointing approximately to the direction of the tag. The start and stop angles of the sector, where the tag responded were recorded. The bearing angle to the landmark was then computed according to the measured sector and the correction parameters related to the antenna and the servo.

The odometry system and the bearing angle measurement system were calibrated before the tests in order to minimize systematic error. The calibration of the bearing angle measurement system indicated, that the expected standard deviation in the bearing angle measurements is  $5^\circ - 10^\circ$  depending on the antenna clearance to the metal parts of the robot and the chosen transmitting power of the RFID reader. During the laboratory experiments it was observed, that depending on the environment the standard deviation can be considerably higher.

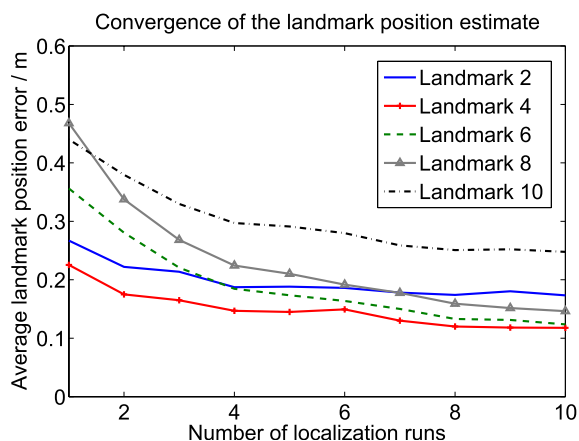


Fig. 6. Accuracy of the final position estimates of the landmarks 2, 4, 6, 8 and 10 as a function of the number of localization runs. The number of runs reflects the number of robots in the group localizing the landmarks, when a true multi-robot system is used. Here, only four robots were available and hence each robot made multiple runs in the scenarios with total number of runs higher than four.

## V. RESULTS

Laboratory experiments with four different robots were conducted. The number of robots is not adequate to prove a true multi-robot performance, but the results of the laboratory measurements were used to tune a simulator to match the real application as closely as possible. In the simulator any number of test runs with any number of robots can be conducted.

### A. Laboratory experiments

Each robot made eight measurement runs. While passing a landmark, the robots made bearing angle measurements on a 20cm interval. The average amount of measurements to a landmark during one pass was approximately six. The odometry and bearing angle measurement information was stored for each measurement run. The localization algorithm could then be run offline with different amount of robots cooperating.

The convergence of five landmark position estimates as a function of the size of the robot group is shown in Figure 6. For each group size, 1000 localization runs were made, where the participating measurement runs were picked from the database of 32 recorded runs. As there were only four robots making the measurement runs, multiple runs per one robot was picked for tests with more than four robots.

The position estimates of all the landmarks converge, as the number of robots and thus, the number of measurement runs increases. The position error of the landmark 10 seems to stay higher than the position error of the other landmarks. This is due to the badly chosen position of the landmark 9, which is too far from the intersection. When a robot turns, the uncertainty of its heading angle estimate increases. A landmark positioned close to the intersection (e.g. landmark 6) offers the robot a reference point for correcting its pose estimate. When turning towards landmark 9, the robot do not have any reference points visible and hence, can not correct its heading. The uncertain heading angle results into accumulated position

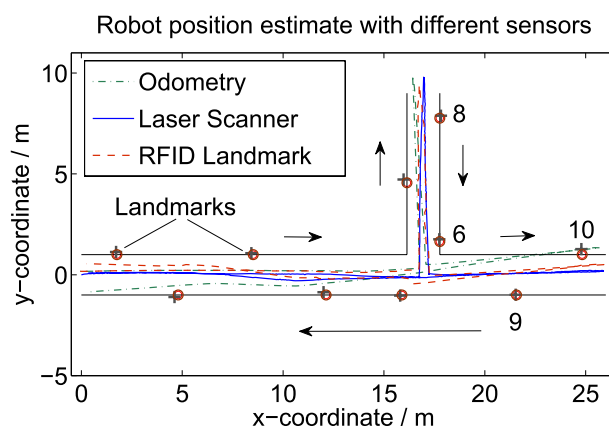


Fig. 7. Robot position estimate with different sensors. Odometry (dash-dot line) shows the estimate based on wheel encoders. Laser scan matching (solid line) serves as reference for ground truth. RFID landmark based estimate (dashed line) shows the performance of the bearing-only localization. True landmark positions are marked with circles and current estimates with crosses. The arrows indicate the robot trajectory direction.

error, which is then inherited by the following landmarks. In addition, the average amount of measurements to landmark 9 was very low (two per pass), due to the disturbances in the environment. Thus, the robot traveled all the way to the landmark 10 with practically no correction to its pose estimate.

The robot position estimate based on different sensors is illustrated in Figure 7. The position estimate based on odometry only shows clearly, how the accumulated error in the robot heading angle estimate causes considerable error in the robot position estimate. The use of RFID tags as landmarks helps to keep the robot position estimate reasonably accurate. The problem with the landmark 9, as mentioned above, is clearly visible. There is no correction on the robot heading angle after the robot turns towards the landmark 10, as there was no successful measurements to the landmark 9 during this particular run. For reference localization, the robot was also equipped with a laser scanner. The environment was artificially made optimal for scan matching with cardboard boxes on regular intervals serving as observable features. Hence, the trajectory of the robot based on the laser scanner measurements gives a good estimate of the true path of the robot.

The stability of the robot position estimate was observed with an experiment, where a robot made six consecutive measurement runs. The robot position estimate with three different methods is illustrated in Figure 8. Once again it is clear, how the position estimate based on odometry gets inaccurate over time. If the robot uses landmarks with no a priori information (plotted as One robot SLAM), the robot position estimate has considerable error, but the accuracy does not decrease over time. With landmarks localized in advance, the robot position estimate stays accurate during the whole experiment.



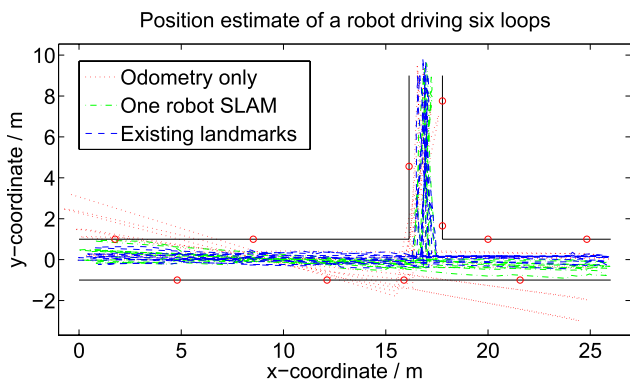


Fig. 8. A robot driving six rounds in the office environment and estimating its position with odometry only (red, dotted line), with bearing-only SLAM (green, dash-dot line) and with already localized landmarks (blue, dashed line).

### B. Simulations

A simulation environment similar to the environment of the laboratory experiments was used. The dimensions of the corridors and the error parameters were approximately the same with the real world system. Ten identical landmarks were positioned evenly over the simulation environment.

The landmark detection depends mainly on the distance between the landmark and the robot. The average number of successful measurements to a landmark during one pass was found to be 5.6, when the measurements were done on 20cm interval. This was modeled in the simulations with the probability function shown in Equation 11, where  $d$  is the real distance between the landmark and the robot.

$$P(\lambda) = \begin{cases} 0.8 & , d < 0.8m \\ 0.5 & , 0.8m \leq d < 1.5m \end{cases} \quad (11)$$

The error distributions for bearing angle measurement and odometry systems were set according to the observed errors during the test runs in the office environment. The values for measurement noises were based on the values used with the real measurement data. The simulations were run in order to observe, how the number of robots affects the localization system performance.

All the robots followed the same path, but the driving direction was different for every other robot. The path was approximately the same that was used in the laboratory experiments (Figure 4).

The landmark position estimate was found to converge towards the correct location as the number of robots contributing increased (Figure 9). The convergence rate depends on the distance from the starting point of the robots (Table I). As the distance increases the error in the heading angle of the robot causes the position error of the robot to increase. This error is inherited by the landmarks, when a robot localizes them. With larger number of robots the average heading angle error approaches zero and thus the position estimates of the landmarks further away from the starting point of the robots become more accurate.

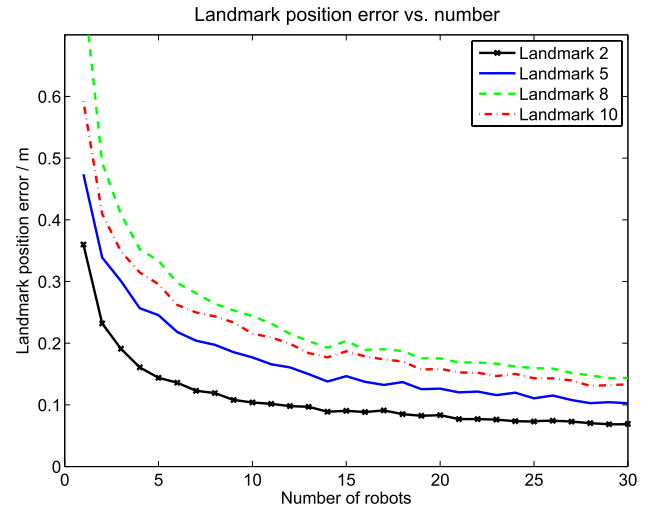


Fig. 9. Landmark position estimate convergence as a function of the number of robots

TABLE I  
 LANDMARK DISTANCE FROM THE STARTING POINT OF THE ROBOTS IN THE SIMULATION ENVIRONMENT AND THE AVERAGE POSITION ERROR OF THE LANDMARK AFTER TEN ROBOTS.

Landmark number	2	5	8	10
Distance from start / m	8	20	32	28
Error after 10 robots / m	0.11	0.18	0.24	0.21

In another simulation, ten runs were made with a single robot and the results were compared to a team of ten robots each making one run. In the single robot case the robot was repositioned after each run, so the odometry error only accumulated over one run and then got set back to the initial values. The robots of the team started from the same position with short intervals and thus there was multiple robots operating simultaneously. The average error in the landmark positions, the average error of a robot after each test run and the average error of a robot when near landmark 8 and landmark 10 (32m and 28m from starting point) were recorded. The results are presented in Table II.

The landmark positions can be estimated more accurately using the multi-robot approach. Also, the robot position estimates have smaller average error and smaller standard deviation if multiple cooperating robots are used. The cooperation helps to keep the error in the robot's pose estimate within smaller margins than what a single robot can do. The increase in the pose error has negative effect on the performance of the Extended Kalman Filter as it uses linearization at the estimated state for the update calculations. The use of multiple robots reduces the effect of systematic errors in the odometry and bearing angle measurement systems of the robots. For reference, a simulation with same error parameters were run on robots with odometry sensors only. The average error in final position was found to be 0.90m, which is clearly higher than the average position error of the robots using the landmarks for localization.

TABLE II  
 LANDMARK AND ROBOT POSITION ERROR WITH SINGLE- AND  
 MULTI-ROBOT LOCALIZATION

	Single-robot		Multi-robot	
	Error	Std dev	Error	Std dev
Landmark final position	0.15m	0.04m	0.14m	0.04m
Robot final position	0.25m	0.30m	0.22m	0.14m
Robot after landmark 10	0.37m	0.24m	0.31m	0.19m
Robot after landmark 8	0.41m	0.26m	0.33m	0.18m

## VI. CONCLUSION

The external localization network clearly supports the localization of the robots, even if the landmark position estimates are not as accurate as with landmarks, that have been manually installed and localized. The estimation error of the robot position is shown to be bounded on a constrained working area, even if there is no a priori information on the positions of the landmarks on that area.

The landmark localization can be done with one or multiple robots. Multiple robots can localize the landmarks with smaller position error and variance. The robots of a cooperating robot group also maintain more accurate estimates of their own position and the variance between robots is considerably smaller. Also the multi-robot approach is significantly faster as all the robots can operate simultaneously.

If the use of robots is not feasible, human operated platforms can be used for the landmark localization instead. The platforms need the same sensors for odometry and bearing angle measurements as the robots. The platforms can be pushed by humans operating at the area or they can be teleoperated, when remote operation is required.

The dimensions of the localization network affect the average convergence of the landmark position estimates. In order to get all landmarks localized with certain accuracy, the amount of robots or independent measurement runs has to be scaled according to the dimensions of the working area as the landmarks further away from the starting point of the robots converge slower.

## VII. FUTURE WORK

The bearing angle measurement system was found to be slow and the accuracy was found mediocre. Alternative or improved methods have to be considered for measuring the bearing angle to a passive RFID tag. The direction of the antenna radiation pattern could be controlled electronically, if an antenna array is used. Also, a different sensor, such as a panoramic camera could be used for the bearing angle measurement.

The distribution of the localization algorithm on the individual robots and the running of the algorithm online is yet to be done. The testing of the communication over an ad-hoc network or through the landmarks could also provide information on the feasibility of this kind of approach. The actual multi-robot experiment with a group of robots operating simultaneously also requires the implementation of suitable systems for collision avoidance and path planning.

## REFERENCES

- [1] E. D. Nerurkar and S. I. Roumeliotis, "Power-slam: A linear-complexity, consistent algorithm for slam," in *International Conference on Intelligent Robots and Systems, 2007. IROS 2007*, 2007, pp. 636–643.
- [2] R. Smith, M. Self, and P. Cheeseman, *Estimating uncertain spatial relationships in robotics*, ser. Autonomous robot vehicles. Springer-Verlag New York, Inc., 1990, pp. 167–193.
- [3] P. Newman and K. Ho, "Slam-loop closing with visually salient features," in *Robotics and Automation, 2005. ICRA 2005. Proceedings of the 2005 IEEE International Conference on*, 2005, pp. 635–642.
- [4] S. B. Williams, G. Dissanayake, and H. Durrant-Whyte, "An efficient approach to the simultaneous localisation and mapping problem," in *Robotics and Automation, 2002. Proceedings. ICRA '02. IEEE International Conference on*, vol. 1, 2002, pp. 406–411 vol.1.
- [5] M. Montemerlo, "Fastslam: A factored solution to the simultaneous localization and mapping problem," in *Proceedings of the AAAI National Conference on Artificial Intelligence*. AAAI, 2002, pp. 593–598.
- [6] R. Kurazume, S. Nagata, and S. Hirose, "Cooperative positioning with multiple robots," in *Robotics and Automation, 1994. Proceedings., 1994 IEEE International Conference on*, 1994, pp. 1250–1257 vol.2.
- [7] I. Rekleitis, G. Dudek, and E. Milios, "Probabilistic cooperative localization and mapping in practice," in *Robotics and Automation, 2003. Proceedings. ICRA '03. IEEE International Conference on*, vol. 2, 2003, pp. 1907–1912 vol.2.
- [8] Y. S. Hidaka, A. I. Mourikis, and S. I. Roumeliotis, "Optimal formations for cooperative localization of mobile robots," in *Robotics and Automation, 2005. ICRA 2005. Proceedings of the 2005 IEEE International Conference on*, 2005, pp. 4126–4131.
- [9] L. A. A. Andersson and J. Nygards, "On utilizing geometric formations for minimizing uncertainty in 3 robot teams," *Robotics / Autonomous Mechanical Systems*, Linkping University, Tech. Rep., 2008.
- [10] A. Howard, L. E. Parker, and G. S. Sukhatme, "The sdr experience: Experiments with a large-scale heterogenous mobile robot team," in *9th International Symposium on Experimental Robotics*, 2004.
- [11] H. J. Chang, C. S. G. Lee, Y. C. Hu, and Y.-H. Lu, "Multi-robot slam with topological/metric maps," in *Intelligent Robots and Systems, 2007. IROS 2007. IEEE/RSJ International Conference on*, 2007, pp. 1467–1472.
- [12] X. S. Zhou and S. I. Roumeliotis, "Multi-robot slam with unknown initial correspondence: The robot rendezvous case," in *Intelligent Robots and Systems, 2006 IEEE/RSJ International Conference on*, 2006, pp. 1785–1792.
- [13] S. Thrun and Y. Liu, "Multi-robot slam with sparse extended information filters," in *Proceedings of the 11th International Symposium of Robotics Research (ISRR'03)*. Sienna, Italy: Springer, 2003.
- [14] R. Martinez-Cantin, J. A. Castellanos, and N. de Freitas, "Multi-robot marginal-slam," *IJCAI Workshop on Multi-Robotic Systems for Societal Applications*, 2007.
- [15] A. Kleiner, J. Prediger, and B. Nebel, "Rfid technology-based exploration and slam for search and rescue," in *Intelligent Robots and Systems, 2006 IEEE/RSJ International Conference on*, 2006, pp. 4054–4059.
- [16] O. Kubitz, M. Berger, M. Perlick, and R. Dumoulin, "Application of radio frequency identification devices to support navigation of autonomous mobile robots," in *Vehicular Technology Conference, 1997 IEEE 47th*, vol. 1, 4-7 1997, pp. 126 –130 vol.1.
- [17] J. Bohn, "Prototypical implementation of location-aware services based on super-distributed rfid tags," in *Proceedings of the 19th International Conference on Architecture of Computing Systems (ARCS06), Frankfurt am Main, Germany. Number 3894 in LNCS, Springer-Verlag*. Springer, 2006, pp. 69–83.
- [18] Herianto, T. Sakakibara, and D. Kurabayashi, "Artificial pheromone system using rfid for navigation of autonomous robots," *Journal of Bionic Engineering*, vol. 4, no. 4, pp. 245 – 253, 2007.
- [19] D. Hahnel, W. Burgard, D. Fox, K. Fishkin, and M. Philipose, "Mapping and localization with rfid technology," in *Robotics and Automation, 2004. Proceedings. ICRA '04. 2004 IEEE International Conference on*, vol. 1, 2004, pp. 1015–1020 Vol.1.